

# Self-Assembly of a Lamellar ABC Triblock Copolymer Thin Film

Kenji Fukunaga\*

UBE Industries, Ltd., 8-1 Goi-minamikaigan, Ichihara, Chiba 290-0045, Japan

Takeji Hashimoto\*

Department of Polymer Chemistry, Graduate School of Engineering, Kyoto University, Kyoto 606-01, Japan

Hubert Elbs and Georg Krausch

Lehrstuhl für Physikalische Chemie II, Universität Bayreuth, D-95440 Bayreuth, Germany

Received October 30, 2001

**ABSTRACT:** We study the self-assembly in thin films of a lamella-forming polystyrene-*block*-poly(2-vinylpyridine)-*block*-poly(*tert*-butyl methacrylate) triblock copolymer by means of scanning force microscopy (SFM) and cross-sectional transmission electron microscopy (TEM). We follow the time development of the microdomain structure in the films during solvent vapor treatment. After preparation on a polar substrate preferentially attracting the middle block of poly(2-vinylpyridine), the films exhibit a spongelike microdomain morphology. With subsequent solvent vapor treatment, metastable lamellae with the spacing much smaller than the equilibrium value are first formed from free surface and grow toward the substrate and eventually establishes a multilayered structure throughout the film. As a result of this process, defects associated with the lamellar structure are annihilated from the free surface and accumulated close to the solid substrate. On an extended solvent vapor treatment, the lamellae thicken toward the equilibrium value. This lamella thickening is accompanied by *autophobic* dewetting of the thin film.

## I. Introduction

There is a growing interest in block copolymers mainly due to their potential to self-assemble into highly ordered structures of mesoscopic scales.<sup>1</sup> In these materials, two or more homopolymer chains are covalently bonded at their chain ends, and the interplay between the molecular connectivity between or among different block chains and repulsive segmental interactions between or among them gives rise to a variety of microphase-separated morphologies after an appropriate thermal equilibration.<sup>2</sup> The presence of external interfaces can significantly influence the resulting microdomain morphologies, especially in thin films, as the component with the lowest interfacial energy may accumulate at the respective interface, thereby aligning the microdomains.<sup>3</sup> In symmetric diblock copolymers, this alignment often leads to a "thickness quantization" of the thin film.<sup>4</sup> When the thickness of the film is not commensurate to the equilibrium lamellar spacing, either holes or islands are nucleated on the film surface to adjust the local film thickness to the preferred quantized values. When the interaction with the surface is significantly reduced, a thickness incommensuration may lead to perpendicular orientation of the lamellae with respect to the boundary surfaces.<sup>5</sup>

While a large number of studies have been reported on thermally equilibrated thin films of AB diblock copolymers and of ABA triblock copolymers, less is known about the self-assembly in thin ABC triblock terpolymer films. Bulk studies on the microphase-separated structure of ABC triblock terpolymers have revealed a rich variety of rather complex morphologies.<sup>6</sup> In contrast to the situation of (sufficiently low molecular weight) diblock copolymers, for terpolymers of more complex architecture thermal annealing does not necessarily provide a successful route for the system to

achieve thermodynamic equilibrium. This is partly due to the high viscosity of the terpolymers and the rather narrow temperature window between the highest glass transition and the lowest thermal degradation temperature of the respective blocks. This is also due to a severe kinetic barrier for a complex metastable structure sometimes formed during sample preparation processes to overcome in order to achieve its equilibrium structure. This barrier arises from strong segregation powers among different block chains. Therefore, swelling the systems with nonselective solvents, followed by drying the systems, has become an effective alternative route for "equilibration".<sup>7,8</sup> Although the solvent treatment has been widely used, the relevant parameters (temperature, solvent vapor pressure, etc.) of this treatment are usually not well controlled, and details of this equilibration process are not well understood yet.

In the present work, we investigate the microdomain morphology in thin films of an ABC triblock terpolymer with nearly symmetric composition "annealed" by solvent vapor swelling and subsequent drying. We use a substrate, which preferentially attracts the middle block of the ABC triblock terpolymer. Therefore, lamellar alignment parallel to the substrate is not expected.<sup>9</sup> If the middle block has the highest surface energy, a parallel alignment of the lamellae is favored in the thin film. We follow the surface induced microdomain alignment as a function of time during the solvent vapor treatment.

## II. Experimental Section

**II.1. Materials.** The polystyrene-*block*-poly(2-vinylpyridine)-*block*-poly(*tert*-butyl methacrylate) triblock copolymers, referred to SVT terpolymer, used in this work were synthesized by sequential living anionic polymerization of styrene, 2-vinylpyridine, and *tert*-butyl methacrylate monomers using *sec*-butyllithium as initiator.<sup>10</sup> The molecular parameters of the

Table 1<sup>a</sup>

	$M_w$	$M_w/M_n$	$\phi_{PS}$	$\phi_{PVP}$	$\phi_{PtBMA}$
SVT1	293 000	1.14	0.18	0.39	0.43
SVT2	172 000	1.10	0.20	0.34	0.46

<sup>a</sup>  $\phi_i$  represents volumetric fraction.

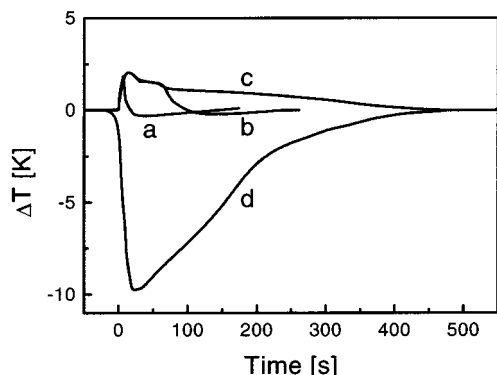


**Figure 1.** Temperature shift  $\Delta T$  of the sample subjected to the THF vapor treatment for 5 s (a), 1 min (b), and 3 days (c). (d) shows  $\Delta T$  during the dipping-and-drying process.

materials are shown in Table 1. SVT1 and SVT2 have different molecular weights but nearly the same composition. Both triblock terpolymers exhibit a lamellar morphology in bulk.<sup>11</sup> In this article, we mainly focus on the results obtained for SVT1. Therefore, in the following results presented without further annotation refer to SVT1.

**II.2. Film Preparation.** Thin SVT triblock terpolymer films were deposited onto native oxide ( $\text{SiO}_2$ ) covered silicon wafers by dip coating from a 0.7 wt % solution in tetrahydrofuran (THF). The samples were pulled out at a velocity of about 10 mm/s. THF is a common solvent to the constituent components for the SVT triblock terpolymer.<sup>12</sup> The thickness of the polymer films used in the present study was 260 nm. The thickness was determined by ellipsometry.

For equilibration the sample was exposed to saturated THF vapor in a closed chamber kept at room temperature for different periods. During the solvent vapor treatment, the macroscopic shape of the film was checked by optical microscopy. In-situ ellipsometry was used to estimate the degree of swelling during the THF vapor exposure. The thin films were swollen to about 113% of the dry film thickness during the first minute. Subsequently, the film thickness gradually increased to about 225% of the dry thickness after about 10 min exposure time. Thereafter, the degree of swelling increased only very slowly. Accordingly, the concentration of the triblock terpolymer in the swollen films decreased to some 88% at 1 min and to about 44% after 10 min. Note that prolonged exposure to saturated THF vapor eventually leads to dewetting of the swollen polymer film from the substrate and thereby to macroscopic fragmentation of the films. After a certain duration of the treatment, the sample was removed to ambient atmosphere and promptly dried.

As changes in the sample temperature may as well affect the microdomain ordering, the temperature was measured by thermocouples attached to some of the specimens. Prior to the dipping process, the thermocouple was bonded to the corner of the silicon substrate by epoxy resin. Thereafter, a thin SVT triblock terpolymer film was deposited in the neighborhood of the thermocouple. The temperature measured by the thermocouple was acquired as a function of time. In Figure 1, the sample temperature shift from room temperature,  $\Delta T = T_{\text{sample}} - RT$ , is shown. Curves a, b, and c represent  $\Delta T$  as a function of time  $t$  during a THF vapor treatment for 5 s, 1 min, and 3 days, respectively. Figure 1 also includes the time dependence of  $\Delta T$  during a dipping process (curve d). For curve d, the time zero represents the time instance when the sample was removed from the solution. For all cases, the sample temperature resumed ambient temperature after about 500 s. The

sharp  $\Delta T$  drop in curve a and b (after 5 and 60 s, respectively) is due to the termination of the treatment (evaporation of the solvent). Without the solvent evaporation (curve c), the sample temperature sharply increases during the first 5 s of the solvent vapor treatment and slowly reaches a maximum after about 10 s followed by a gradual decrease to room temperature. The sample is slightly heated by the latent heat gained during solvent condensation, whereas the sample is cooled in the thin film deposition by the latent heat loss due to the solvent evaporation.

**II.3. Scanning Force Microscopy (SFM).** The samples were investigated by TappingMode SFM (Nanoscope III, Digital Instruments, Santa Barbara, CA).<sup>13</sup> All SFM measurements were performed in ambient atmosphere. Silicon tips with a tip curvature of some 5–10 nm (Nanosensors, Germany) were used.

**II.4. Transmission Electron Microscopy (TEM).** Some portions of the respective samples were removed from the silicon substrate for TEM inspection. For this purpose, the samples were first soaked in aqueous KOH solution (pH 12) at 70 °C for a few seconds followed by washing in distilled water at room temperature. This procedure was chosen to overcome the strong adhesion of the films to the substrate. Subsequently, some portions of the film were carefully peeled off the substrate and floated onto distilled water. The floating films were picked up onto a polyimide sheet and dried. The films on the polyimide support were then embedded in light-curing acrylic agent (Luxtrak, Toagosei Co., Tokyo, Japan), and the matrix agent was subsequently cured by UV irradiation. During this procedure, the sample was cooled in order to minimize a swelling of the sample by the curing agent. The specimens were trimmed and sliced to 140 nm thickness parallel to the film normal by using an ultra-microtome (ULTRACUT-S, Leica). Finally, the cross-sectional pieces were stained by  $\text{OsO}_4$  vapor. TEM images were taken on a JEM-200CX (JEOL, Japan) microscope.

To check for the potential influence of the KOH treatment on the microstructure of the samples, some specimens were stained by  $\text{RuO}_4$  vapor prior to the KOH treatment. However, this treatment was found not to cause any difference in the final TEM images. Furthermore, the surface topography of the samples as detected by SFM did not show significant changes by the KOH treatment. Consequently, the structure of the thin SVT triblock terpolymer films seems not to be significantly modified by the KOH treatment.

### III. Results

**III.1. Initial Structure.** An SFM height image of the as-prepared film surface is shown in Figure 2a. The image exhibits a macroscopically flat surface except for small protrusions separated by a characteristic spacing. The depth of the protrusions ranges between 3 and 5 nm. The characteristic spacing between the protrusions was determined to be  $70 \pm 15$  nm by Fourier transform of the height image. A cross-sectional TEM image of the as-prepared film is shown in Figure 3a. After staining with  $\text{OsO}_4$ , T, V, and S domains are expected to appear gray, dark, and bright, respectively. In Figure 3, the polyimide substrate (i.e., the interface to the  $\text{SiO}_2$  substrate in the sample preparation) and the embedding acrylic matrix (i.e., the interface to air in the sample preparation) are designated by "S" and "A", respectively. As seen in Figure 3a, the film interior exhibits "spongelike" microphase-separated domains with only short-range order (see Figure 7 of ref 14). The TEM image allows to distinguish three different microphases (dark, gray, and bright), each of which appears to be continuous in space.

The characteristic spacing of the spongelike domains (e.g., spacing of the bright domains) is determined to be  $71 \pm 11$  nm, in good agreement with the spacing of

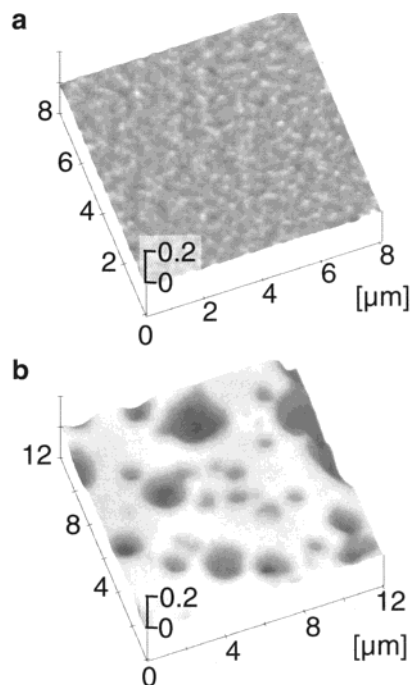


**Figure 2.** SFM height image of the as-prepared film (a) and of the film subjected to the THF vapor treatment for 1 min (b). Note that the lateral scale is different for each image: 8  $\mu\text{m}$  (a) and 12  $\mu\text{m}$  (b). The vertical axis represents the height measured from the substrate surface in  $\mu\text{m}$ .

the surface corrugations (see Figure 2a). For a direct comparison of SFM and TEM data, we display an SFM height image of higher magnification (Figure 4a) together with cross-sectional TEM images of the interior (Figure 4b) and of the near-surface region of the films (Figure 4c). Obviously, the surface topography of the as-prepared film shown in Figure 4a somehow reflects the microdomain morphology found in the "bulk" of the thin film. It should be noted however that the surface of the as-prepared film is covered with a continuous layer as seen in Figure 4c. In Figure 4c some undulation in the contour of the topmost layer is found with a characteristic spacing of about 70 nm, which is again similar to that of the surface corrugations observed in the SFM images.

**III.2. Solvent Vapor Treatment. A. Surface-Induced Alignment.** On exposure to THF vapor, the as-prepared SVT triblock terpolymer film immediately develops a stepped surface as can be seen via the interference colors in optical microscopy (not shown here). The interior structure of the sample was inspected by cross-sectional TEM. Figure 3b,c shows the cross-sectional image of the thin film after a THF vapor treatment for 5 s taken at two different spots less (Figure 3b) and more affected (Figure 3c) by the short treatment. The interface between the thin triblock terpolymer film and the acrylic matrix exhibits only a weak contrast in the TEM images. For clarity, we have marked the approximate position of this interface by a dotted line in the figure. Figure 3b,c manifests that even a very short THF vapor treatment leads to the formation of lamellae aligned parallel to the free surface of the film. While some spongelike microdomains are present after the very short vapor treatment, an extended vapor treatment eventually transforms from the spongelike phase into the lamellar phase throughout the entire film. After only 1 min of the THF vapor exposure, a well-ordered multilayered structure has been established in

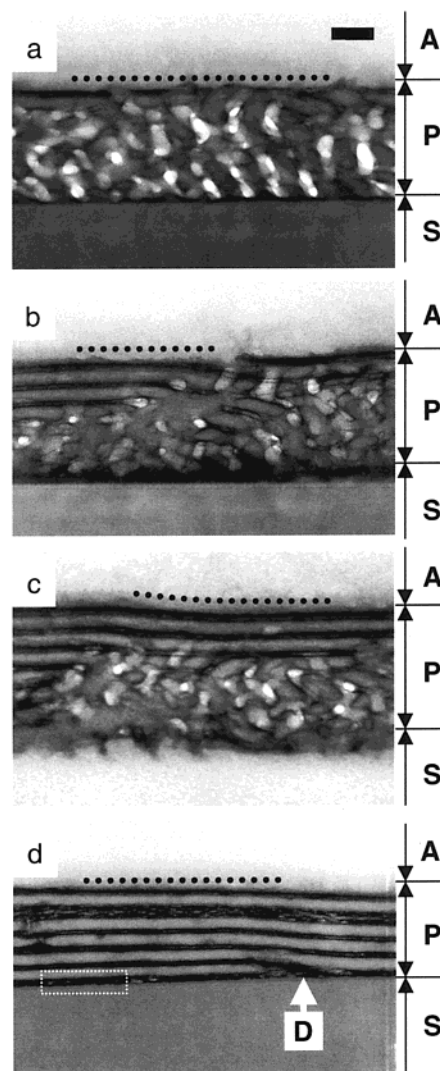


**Figure 3.** Cross-sectional TEM images showing the time evolution of self-assembly in the thin SVT triblock terpolymer film: as-prepared (a), after the THF vapor treatment for 5 s (b, c), and 1 min (d). The black scale bar, common for the all images, in the topmost figure represents 100 nm. The embedding matrix, the substrate, and the triblock terpolymer film are in the portion A, S, and P, respectively. PS, P2VP, and PtBMA microdomains appear bright, dark, and gray, respectively, in the TEM images. Dotted lines represent the approximate position of the free surface in the respective images. In (d), a dislocation core is indicated by D.

the entire film (Figure 3d). The lamellae in Figure 3b–d are zoomed up in Figure 5. The three-phase coexisting lamellae are clearly observed here. The lamellar spacing  $L_{\text{TEM}}$  is found to be  $L_{\text{TEM}} = 40 \pm 5$  nm, which is far less than the bulk lamellar spacing ( $L_{\text{TEM,bulk}} = 111.8$  nm<sup>11</sup>).

The presence of a polar substrate is expected to favor the accumulation of the polar V middle block, thereby leading to a frustration of a parallel alignment of the lamellae at the substrate surface. A portion of the triblock terpolymer film adjacent to the substrate (see Figure 3d, marked by white dotted line) is zoomed up in Figure 6. In this figure, the contrast is enhanced from the original TEM picture by a digital image processor. It shows a row of discontinuous bright domains embedded within a dark layer. The dark layer is supposed to correspond to a V microdomain, whereas the bright domains correspond to either S or T microdomains, which appear in different brightness (S domain brighter).



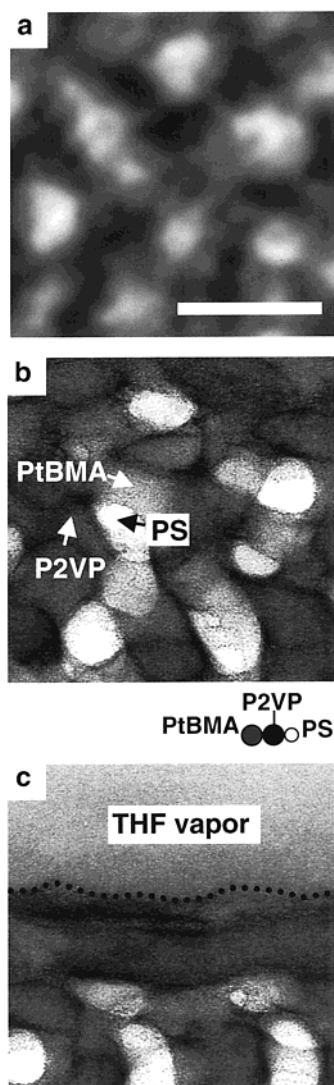


**Figure 4.** Zoom up of the surface topography (a) as observed by SFM and of the interior morphology (b) as observed by the cross-sectional TEM, both for the as-prepared film. A cross-sectional TEM image including the free surface of the film (indicated by the dotted line) is shown in (c). The radius of gyration of each block chain is schematically shown below (b). In the SFM image (a), height is ranging from 0 to 10 nm. The white bar in (a) represents 100 nm and applied for all the images.

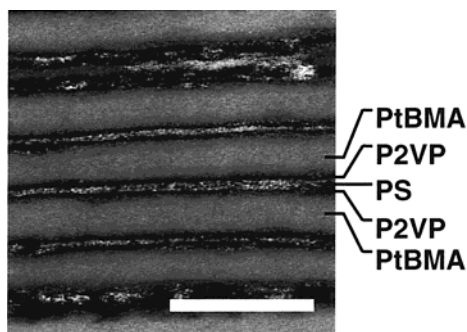


**Figure 5.** Zoom-up of the lamellar structure developed after the THF vapor treatment for 1 min, as observed by the cross-sectional TEM. The white bar represents 100 nm.

The bright discrete domains are located at approximately 10 nm above the substrate with an average interdomain distance parallel to the substrate of about 40 nm.

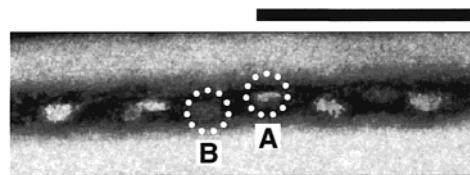


**Figure 6.** Zoom-up of the portion closest to the substrate (see dotted area in Figure 3d), as observed by cross-sectional TEM. The black scale bar represents 100 nm. Note that the contrast is enhanced from the original TEM image. PS and PtBMA domain appear in different contrast (indicated by A and B, respectively).

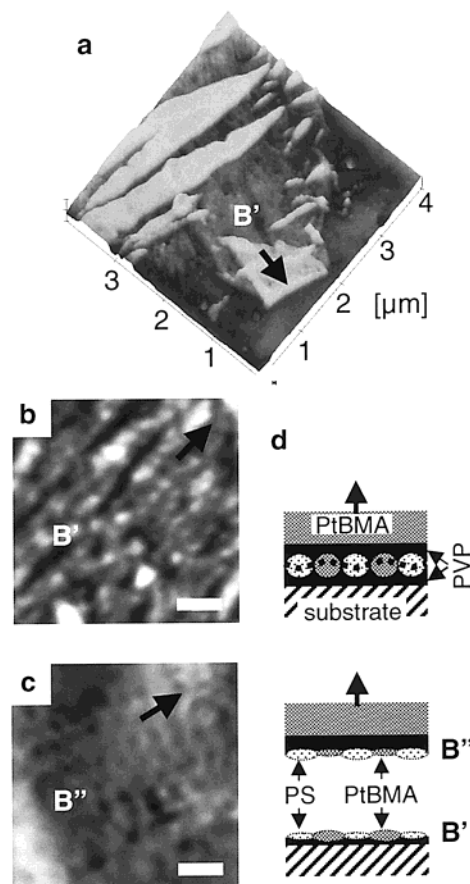


**Figure 7.** SFM height images of fractured surface of a thin SVT triblock terpolymer film firmly adsorbed to the substrate (a). Thin layer (B') left on the substrate is zoomed-up in (b) together with the counter surface (B'') of the fractured film (c). Arrow in (a–c) indicates direction of the fracture. Bar in (b, c) represents 100 nm. The fractured position is schematically illustrated by a dotted line in the upper figure of (d). Schematic diagram after the fracture to B' and B'' is shown in the lower figure of (d).

Further insight into the near-substrate structure of the terpolymer films can be gained by SFM inspection of the portions of the film, which remain firmly adsorbed to the  $\text{SiO}_x$  substrate after the film has been peeled off from the substrate for cross-sectional TEM. In some areas, a thin terpolymer layer is left on the substrate after the peel, indicating that the film has fractured close to the substrate. A typical SFM height image of such a "cleavage surface" of the film adhered to the substrate is shown in Figure 7a. The SFM image shows a thin layer (B') left on the  $\text{SiO}_x$  substrate surrounding the unfractured part of the film. The thickness of this layer is about 10 nm, which corresponds to the height of the discrete domains in the layer adjacent to the

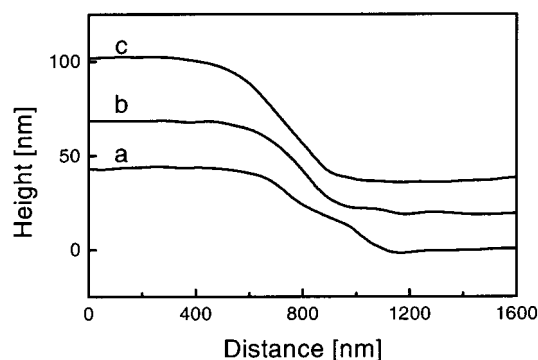


**Figure 8.** Step profile obtained by cross section of SFM height image: the THF vapor treatment for 5 s (a), 1 min (b), and 3 days (c). Curves a–c are vertically shifted for clarity.

substrate shown in Figure 6. A higher magnification SFM image of the region B' in Figure 7a and that of the counter surface of the fracture film (B'') are shown in parts b and c of Figure 7, respectively. In the respective figures, the peeling direction is indicated by an arrow. Beside the defects due to the tensile deformation in the peeling process, isolated rather regular protrusions and depressions are observed on surfaces B' and B'', respectively. These features have a similar characteristic spacing of  $\sim 40$  nm, which coincides with the average interval of the discrete brighter domains in the TEM image (see Figure 6).

Now, let us turn to the macroscopic structure of the multilayered film (Figure 3d). Within the films, we observe regions of different numbers of lamellae. In Figure 3d, the left-hand part of the film contains one extra lamellar layer as compared to the right-hand part. This leads to an edge dislocation like a smectic A liquid crystal film<sup>4</sup> (see Figure 3d, indicated by "D"). Around the dislocation, the thickness of the film is slowly decreasing from the left to the right. The cross-sectional TEM image manifests that the thickness difference across the dislocation is commensurate to the lamellar spacing. An SFM height image of this sample is shown in Figure 2b. The surface appears rather flat except for depressed areas separated by  $\sim 1$   $\mu\text{m}$ . Within the depressions the surface is almost flat as well, and the depressions are enclosed by well-defined steps. Even after THF vapor treatment as short as 5 s, some steps were detected by SFM in a few positions, indicating that the lamellar phase had locally grown to the substrate in these positions. From cross sections of the SFM height image, one can estimate the height of the step. In Figure 8, SFM cross sections of steps formed after 5 s (a) and 1 min (b) THF vapor treatment are shown. Curves b and c are shifted vertically by 20 and 40 nm, respectively. The step developed during the 5 s treatment exhibits rather a gentle slope. After the treatment for 1 min, however, the step has become significantly steeper whereas the total height of the step stays nearly the same. From various steps imaged at different spots of the samples, a step height of  $L_{\text{SFM}} = 40 \pm 5$  nm is found. The step height observed by SFM coincides with the lamellar spacing  $L_{\text{TEM}}$  (see Figure 5) as expected. Therefore, the step observed in the SFM image is supposed to be a signature of the lamellar grain boundary accompanied by the edge dislocation. We note here that, in the present system, the edge dislocation cores were always found in the vicinity of the substrate.

**B. Dewetting of the Thin Films.** On an extended THF vapor treatment, the film starts to dewet from the

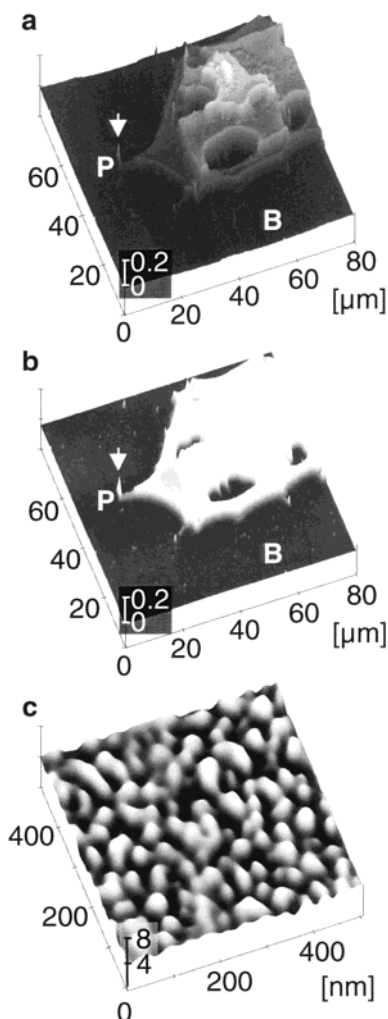


**Figure 9.** SFM height image of a thin SVT triblock terpolymer film after the THF vapor treatment for 3 days (a). In (b), the contrast of this image is adjusted in such a way that the details of the low height areas are visible. The vertical axis in (a, b) represents the height measured from the substrate surface in  $\mu\text{m}$ . The dry patch (B) is zoomed-up in (c), where the vertical axis represents the height measured from the substrate in nm.

substrate. Figure 9 presents a typical SFM height image taken after a 3 day THF vapor treatment. The image shows a region near the contact line between a dewetted dry patch (marked by "B" in Figure 9) on the substrate and the dewetting film. On the film, we find terraces of well-defined thickness separated by rather a steep step of constant height. Compared to the surface features observed after short THF vapor treatment, the lateral dimensions of the terraces have considerably grown to a few tens of micrometers. Moreover, after the long treatment the steps are both steeper and higher as compared to the short treatment (see Figure 8c). The step height increased from 40 to  $\sim 60$  nm. Note that some terraces exhibit tentacle-shaped tails (marked by "P" in Figure 9b). These tails are possibly due to pinning of the contact line during the dewetting motion of the film. The contact line pinning is often caused by dust particles or some damages on the substrate.<sup>15</sup> In fact, as indicated by a white arrow in Figure 9, dust particles are frequently found on the apexes of the tails. The dry patch (B), magnified in Figure 9c, is covered by an ultrathin film of the triblock terpolymer as observed before.<sup>12</sup> It resembles the *autophobic* dewetting which

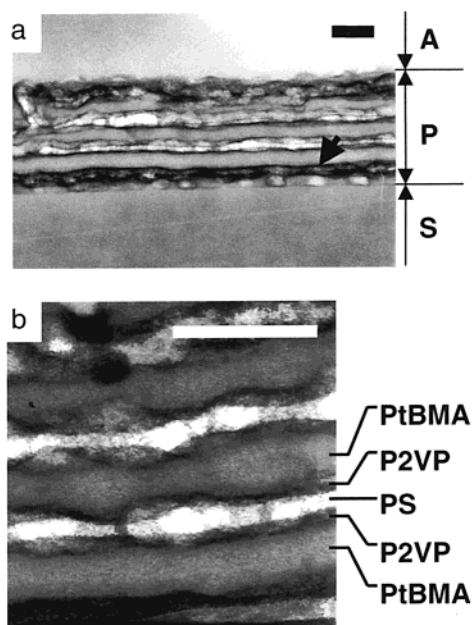


**Figure 10.** Cross-sectional TEM images of a thin SVT triblock terpolymer film after the THF vapor treatment for 3 days (a). The interior lamellae are magnified in (b). The bar in the respective image represents 100 nm. A, P, and S have the same meaning as in Figure 3. The black arrow indicates the layer with the discrete bright domains (see text).

has been reported on thin films of some block copolymer systems.<sup>16</sup>

The internal structure of the films after the extended THF vapor treatment was investigated by cross-sectional TEM (Figure 10a). Again, lamellae aligned parallel to the film surface are observed. Figure 10b shows a higher magnification image of the lamellae in Figure 10a. Quantitative comparison of Figures 5 and 10b reveals that the lamellae thicken during the prolonged THF vapor treatment. The lamellar spacing found in Figure 10b is  $60 \pm 5$  nm, in good agreement to the step heights observed by SFM. Yet, the lamellar spacing found in Figure 10 is still far below the bulk spacing. Note that the internal interfaces of the thickened lamellae are rather meandered compared to those for the short treatment case.

We note that the structure of the layer adjacent to the substrate has improved during the long-term THF vapor treatment. Similar to the TEM image (Figure 3d) taken for the sample with the short treatment, a layer with discrete bright domains (indicated by the black arrow in Figure 10a) is seen in the vicinity of the substrate after the long treatment as well. In Figure 10a, one can clearly distinguish bright (S) domains separated by gray (T) domains adjacent to the substrate, whereas the structure in this region was only poorly developed after the short treatment (see Figure 3d). The interface to the substrate appears slightly dark in the image, indicative of V chains adsorbed onto the  $\text{SiO}_x$  surface. The thickness of the inhomogeneous layer adjacent to the substrate is  $\sim 20$  nm in Figure 10a, which is considerably larger than that in Figure 3d. We tried to investigate the "cleavage surface" similar to the experiments described after the short-term treatment (Figure 7). However, it turned out that the adsorbed layer was not preferentially fractured in this case. This suggests that the rearrangement of the adjacent layer lead to a stronger mechanical link within the block copolymer film.

**III.3. Thin Films of Lower Molecular Weight Copolymer.** We have performed a similar set of experiments on the lower molecular weight SVT2 triblock terpolymer. We find that the swelling rate as well as the temperature shift profile of SVT2 during solvent vapor treatment is nearly identical to SVT1. In contrast to the higher molecular weight SVT1 case, however, the entire process of microdomain ordering is considerably faster. In the as-prepared sample, the multilayered lamellar structure has already formed. Some lamellae thickening is observed on longer solvent vapor exposure as well, however on time scales of seconds rather than minutes. This finding seems reasonable given the lower viscosity expected for lower molecular weight chains. Since no qualitatively new insights are to be gained from these experiments, we will not discuss them in further detail in the following.

#### IV. Discussion

The cross-sectional TEM images taken on the as-prepared samples revealed a spongelike distorted microphase-separated structure (Figure 3a). This structure is a snapshot of the vitrified polymer solution and most likely represents a kinetically trapped nonequilibrium state, where T-blocks seem to comprise a matrix and the other blocks form continuous structures as schematically shown in Figure 11a. The structure resembles "spongelike" structures observed in diblock copolymer bulk specimens.<sup>14</sup> Interestingly, the free surface of the as-prepared film is covered by a homogeneous layer (Figures 3a and 4c). In multicomponent polymer systems, it is generally observed that the lower surface tension component tends to cover the free surface.<sup>3</sup> In the system studied here, the T-block is the lowest surface free energy component, and hence the free surface is expected to be enriched in this material. The segregation of T end blocks at the free surface triggers the subsequent lamella formation originating at the free surface (see Figure 11a,b).

Upon solvent vapor exposure, the free surface of the thin SVT triblock terpolymer film immediately develops the "smectic" lamellar grains aligned parallel to the surface (see change from Figure 3a to c). In the isotropic bulk, nucleation growth of lamellar grains from a disordered phase has been observed to be anisotropic with the grain size along the lamellar normal being much larger than that parallel to the lamellar interfaces.<sup>17</sup> Opposite to the bulk case, in Figure 3b,c the growing lamellar grains have a much larger lateral size than thickness. This is an indication that the lamellar microdomains order from the free surface and grow to the "bulk" of the thin film as schematically illustrated in Figure 11b–d. This fact is corroborated by the observed time dependence, clearly revealing that the lamellae start growing at the free surface of the film. In this respect, our findings closely resemble the well-known surface-induced alignment of the lamellar microdomains observed on thermally equilibrated thin films of symmetric diblock copolymers.<sup>18</sup>

In contrast to the case of thin diblock copolymer films, where formation of lamellae typically originate at either of the boundary surfaces, in the case of SVT the  $\text{SiO}_x$  substrate surface seems not to induce ordering of the lamellae. Poly(2-vinylpyridine) is known to strongly adsorb to  $\text{SiO}_x$  surfaces.<sup>12</sup> Following recent mean-field calculation results by Pickett and Balazs,<sup>9</sup> it is expected under these conditions that the two end blocks are



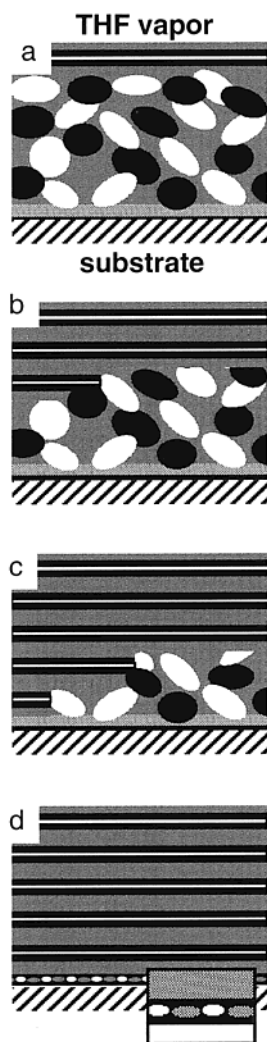


**Figure 11.** Schematic diagram of self-assembly of the microdomains in the thin SVT triblock terpolymer film. The as-prepared film has sponge-like distorted microdomain structure in the bulk with a homogeneous layer of PtBMA on the free surface. The homogeneous layer triggers the surface-induced ordering into the three-phase coexisting lamellae. Upon the THF vapor treatment, the lamellar grains first formed at the free surface are grown to bulk of the film (b, c) and finally to the lamellae with a uniform multilayered structure throughout the film (d). Because of strong interactions of middle block to the substrate, a laterally microphase-separated structure (inset of d) is formed in the region adjacent to the substrate (see text).

microphase-separated to form a heterogeneous structure along the film plane. This expectation is indeed confirmed experimentally. As shown in Figures 6 and 10a as well as in Figure 7, in the immediate vicinity of the substrate surface, a laterally inhomogeneous morphology is observed. This findings compares well to recent experiments on *ultrathin* SVT triblock terpolymer films, revealing a complex in-plane structure on the film surface, where isolated protrusions of S and of T blocks were observed on top of the layer of V block adsorbed to the substrate.<sup>12</sup> A similar in-plane structure is observed on the “cleavage surface” of the SVT triblock terpolymer films in the present study (Figure 7). Since all components are glassy at room temperature, the fracture is supposed to proceed through the laterally inhomogeneous region which includes weak mechanical links (e.g., chain ends) as schematically depicted in Figure 7d. The dotted line in the upper figure illustrates

schematically the fractured position, and the lower part of the figure shows a schematic diagram after the fracture. Hence, the granular topography on the fracture surface (Figure 7b,c) reflects the ordering into S and T microdomains in the region adjacent to the substrate. We therefore conclude that the structure of this region comprises isolated microdomains of S and T embedded in the center of the lamellar microdomain of V blocks (see the inset in Figure 11d). Furthermore, the particular microphase-separated structure adjacent to the substrate was not immediately developed by the THF vapor treatment, and it became visible after 1 min (see Figure 3d). The strong adsorption of V blocks to the substrate seems to kinetically suppress the microdomain ordering near the substrate. Because of this suppression, the growing lamellar structure is faced to its commensurability near the substrate. Therefore, the defects associated with the thickness incommensuration may be mostly formed in the region near the substrate.

After the vapor exposure for 1 min, the three-phase lamellae are uniformly developed with their interfaces parallel to the surface of the thin film (defined as the “first stage” ordering process). After a further prolonged THF vapor treatment, a thickening of the lamellar microdomains was observed in the present system (defined as the “second stage” ordering process). Here, one may ask whether the second stage is controlled thermodynamically. During the THF vapor treatment, the polymer concentration  $\phi$  in the thin film varies considerably with the treatment time. Hashimoto and co-workers<sup>19</sup> found that the microdomain spacing  $L$  in the solution scales as  $L = L_0(\phi T_0/T)^{1/3}$ , where  $L_0$  is an equilibrium lamellar spacing in bulk ( $\phi = 1$ ) at temperature  $T_0$ . The temperature  $T$  is read from Figure 1, and the concentration  $\phi$  is determined by ellipsometry as described in section II.2 both as a function of time during the vapor treatment. Using the scaling law given above,  $L_{1\text{ min}} = 107\text{ nm}$  is calculated from  $T = 300\text{ K}$  and  $\phi = 0.88$ , both of which were measured after the solvent vapor treatment for 1 min. Here  $L_0 = 111.8\text{ nm}$  is assumed<sup>11</sup> at  $T_0 = 298\text{ K}$  and at  $\phi = 1$ . As for the solvent vapor treatment for 3 days, we do not have an experimental value of the  $\phi$  due to the macroscopic fragmentation of the sample. However, we may replace the value of  $\phi$  for the 3 day treatment by the value of  $\phi = 0.44$  obtained after the solvent vapor treatment for 10 min, since the swelling degree of the film very slowly increased after the vapor treatment for 10 min. The actual  $\phi$  after the long treatment is considered smaller than this value. Hence,  $L_{3\text{ day}} = 85\text{ nm}$  calculated from  $T = 298\text{ K}$  and  $\phi = 0.44$  gives the upper limit of the expected lamella spacing after the solvent vapor treatment for 3 days. Because of the solvent removal before the observation in the present study, these estimated values do not directly correspond to the observed ones. Qualitatively, however, the lamellar spacing is expected to be unchanged during the rapid solvent removal process, and the lamellar spacing in the vapor treated thin film should decrease with increasing treatment time as indicated in the expected variation from  $L_{1\text{ min}}$  to  $L_{3\text{ day}}$ , contrary to the experimental observation where the lamellar spacing increased from 40 nm (Figure 5) to 60 nm (Figure 10). Therefore, we propose the following scenario for the observed thickening of the lamellae.

Constraints in the thin film induced by the boundary surfaces may suppress the establishment of the equilibrated lamellar microphase in the first-stage ordering

process induced by the short-term solvent vapor exposure. Hence, uniformly formed lamellae in the first stage are expected to have the spacing much smaller than the equilibrium value. The bulk free energy cost of the nonequilibrium microphase must be minimized in the second-stage ordering process induced by the long-term vapor treatment. The lamellar thickening observed in this second-stage ordering process involves an increase in the areal density of the junction points of the triblock terpolymer. Therefore, this process reduces the interfacial area per volume and hence the free energy of the system. At the same time, the multilayered film macroscopically shows the *autophobic* dewetting which is indicative of reducing of the lamellar interfaces. Generally, the chain diffusion is considerably faster in the direction along the microdomain interfaces than in the direction across the microdomain interfaces.<sup>1</sup> Hence, the reduction of the lamellar interfaces is expected to be caused by the diffusion of the junction points along the lamellar interfaces.

## V. Conclusion

In this study, the thin film structure of SVT triblock terpolymers on a polar substrate is investigated by means of both SFM and cross-sectional TEM. As-prepared films exhibit a trapped spongelike microphase-separated structure covered by a thin homogeneous layer of the lowest surface energy component on the free surface. The free surface topography reflects the interior spongelike morphology. Upon "annealing" with THF vapor, lamellae develop originating from the free surface of the film. Eventually, the lamellae are developed throughout the entire film. In the region near the substrate, a thin, laterally inhomogeneous microphase-separated layer is formed, which allows the polar middle block to adsorb at the polar substrate. After the prolonged treatment, the nonequilibrium lamellar microdomains are annealed to thicker equilibrated ones. This late process is accompanied by macroscopic dewetting of the film from the substrate, resulting in thickening of the film.

**Acknowledgment.** The authors gratefully acknowledge financial support through the Deutsche Forschungsgemeinschaft (SFB 481) and the Ministry of Science, Sports, and Culture, Japan (A 12305060). We are grateful to R. Stadler, V. Abetz, and E. Giebler for supply of the block copolymers and for helpful discussions during the experimental work. We also thank to K. Itoh for technical help for TEM observations.

## References and Notes

- (1) Bates, F. S.; Fredrickson, G. H. *Annu. Rev. Phys. Chem.* **1990**, *41*, 525.
- (2) Khandpur, A. K.; Förster, S.; Bates, F. S.; Hamley, I. W.; Ryan, A. J.; Bras, W.; Almdal, K.; Mortensen, K. *Macromolecules* **1995**, *28*, 8796.
- (3) Hasegawa, H.; Hashimoto, T. *Macromolecules* **1985**, *18*, 589.
- (4) Liu, Y.; Rafailovich, M. H.; Sokolov, J.; Schwarz, S. A.; Bahal, S. *Macromolecules* **1996**, *29*, 899.
- (5) Kellogg, G. J.; Walton, D. G.; Mayes, A. M.; Lambooy, P.; Russell, T. P.; Gallagher, P. D.; Satija, S. K. *Phys. Rev. Lett.* **1996**, *76*, 2503.
- (6) Zheng, W.; Wang, Z.-G. *Macromolecules* **1995**, *28*, 7215.
- (7) Kim, G.; Libera, M. *Macromolecules* **1998**, *31*, 2569. Kim, G.; Libera, M. *Macromolecules* **1998**, *31*, 2670.
- (8) Albalak, R. J.; Capel, M. S.; Thomas, E. L. *Polymer* **1998**, *39*, 1647.
- (9) Pickett, G. T.; Balazs, A. C. *Macromol. Theory Simul.* **1998**, *7*, 249.
- (10) Giebler, E.; Stadler, R. *Macromol. Chem. Phys.* **1997**, *198*, 3815.
- (11) Giebler, E. Dissertation, Universität Mainz, 1997.
- (12) Fukunaga, K.; Elbs, H.; Magerle, R.; Krausch, G. *Macromolecules* **2000**, *33*, 947.
- (13) Zhong, Q.; Innis, D.; Kjoller, K.; Elings, V. B. *Surf. Sci. Lett.* **1993**, *290*, L688.
- (14) Hashimoto, T.; Koizumi, S.; Hasegawa, H.; Izumitani, T.; Hyde, S. T. *Macromolecules* **1992**, *25*, 1433.
- (15) De Gennes, P. G. *Rev. Mod. Phys.* **1985**, *57*, 827.
- (16) Limary, R.; Green, P. F. *Langmuir* **1999**, *15*, 5617; *Macromolecules* **1999**, *32*, 8167. Hamley, I. W.; Hiscutt, E. L.; Yang, Y.-W.; Booth, C. J. *Colloid Interface Sci.* **1999**, *209*, 255.
- (17) Sakamoto, N.; Hashimoto, T. *Macromolecules* **1998**, *31*, 3815.
- (18) Russell, T. P.; Mayes, A. M.; Kunz, M. S. In *Ordering in Macromolecular Systems*; Teramoto, A., Kobayashi, M., Norisuye, T., Eds.; Springer-Verlag: Berlin, 1994; p 217.
- (19) Hashimoto, T.; Shibayama, M.; Kawai, H. *Macromolecules* **1983**, *16*, 1093.

MA011889M